

Systematic Evaluation of Molecular Recognition Phenomena. 3. Selective Diphosphate Binding to Isomeric Hexaazamacrocyclic Ligands Containing Xylylic Spacers

Carmen Anda,[†] Antoni Llobet,^{*†} Arthur E. Martell,[‡] Bruno Donnadieu,[§] and Teodor Parella^{||}

Departament de Química, Universitat de Girona, Campus de Montilivi 17071, Girona, Spain,
Department of Chemistry, Texas A&M University, College Station, Texas 77843-3255, Service de
Cristal·lochimie, Laboratoire de Chimie de Coordination, UPR CNRS 8241, Route de Narbonne
205, F-31077 Toulouse Cedex 4, France, and Servei de RMN, Universitat Autònoma de
Barcelona, Bellaterra, E-08193 Barcelona, Spain

Received February 24, 2003

The crystal structure of 3,7,11,18,22,26-hexaazatricyclo[26.2.2.2^{13,16}]tetraatriaconta-1(31),13(34),14,16(33),28(32),-29-hexaene hexahydrobromide salt [(H₆P3)Br₆] has been determined by means of X-ray diffraction analysis. It crystallizes with an additional molecule of ethanol and half a molecule of water per molecule of the hydrobromide P3 ligand. The protonation constants of P3 and its host–guest interactions with monophosphate (Ph) and pyrophosphate (Pp) have been investigated by potentiometric equilibrium methods. Ternary complexes are formed in aqueous solution as a result of hydrogen bond formation and Coulombic interactions between the host and the guest; formation constants for all the species obtained are reported and compared with the isomeric 3,7,11,19,23,27-hexaazatricyclo[27.3.1.1^{13,17}]tetraatriaconta-1(33),13, 15,17(34),29,31-hexaene (Bn) ligand. For the H₆P3Pp²⁺ those bonding interactions reach a maximum yielding a log *K*₆^R of 5.87. The selectivity of the P3 ligand with regard to the monophosphate and pyrophosphate substrates (S) is discussed and illustrated with global species distribution diagrams showing a strong preference for the latter over the former as a consequence of the much stronger formation constants with pyrophosphate. An analysis of the isomeric effect is also carried out by comparing the P3–S versus Bn–S systems. In the best case, a selectivity of over 88% is achieved for the diphosphate complexation when using the *meta* isomer over the *para*, due solely to the size and shape of the receptors cavity.

Introduction

The molecular recognition of anionic guest species is an area of current intense chemical investigation^{1–8} with

* To whom correspondence should be addressed. E-mail: antoni.llobet@udg.es.

[†] Universitat de Girona.

[‡] Texas A&M University. E-mail: martell@mail.chem.tamu.edu.

[§] Laboratoire de Chimie de Coordination. E-mail: donadieu@lcc-toulouse.fr.

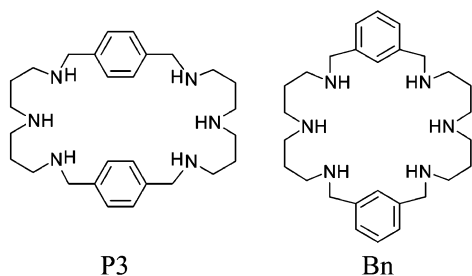
^{||} Universitat Autònoma de Barcelona. E-mail: teo@rnm4.uab.es.

- (1) (a) Beer, P. D. *Chem. Commun.* **1996**, 689. (b) Beer, P. D. *Acc. Chem. Res.* **1998**, *31*, 71. (c) Beer, P. D.; Gale P. A. *Angew. Chem., Int. Ed.* **2001**, *40*, 487. (d) *Supramolecular Chemistry of Anions*; Bianchi, A., Bowman-James, K., García-España, E., Eds.; John Wiley & Sons: Chichester, U.K., 1997. *Supramolecular Chemistry*; Steed, J. W., Atwood, J., Eds.; John Wiley & Sons: Chichester, U.K., 2000.
- (2) (a) Gerasimchuk, O. A.; Mason, S.; Llinares, A. M.; Song, M.; Alcock, N. W.; Bowman-James, K. *Inorg. Chem.* **2000**, *39*, 1371. (b) Clifford, T.; Danby, A.; Llinares, J. M.; Mason, S.; Alcock, N. W.; Powell, D.; Aguilar, J. A.; García-España, E.; Bowman-James, K. *Inorg. Chem.* **2001**, *40*, 4710.

potential applications in areas such as the designing of positively charged or electron-deficient neutral abiotic organic receptor molecules.

Within this field, we have recently undertaken a systematic evaluation of molecular recognition phenomena between phosphates and nucleotides on the basis of hexaazamacrocyclic ligands containing *m*-xylylic and diethylic ether spacers.⁹ In that work, we have quantitatively evaluated the different factors involved in the recognition processes, namely, Coulombic, hydrogen bonding, and π – π stacking interactions.

- (3) (a) He, H.; Martell, A. E.; Motekaitis, R. J.; Reibenspies, J. H. *Inorg. Chem.* **2000**, *39*, 1586. (b) Kong, D. Y.; Martell, A. E.; Motekaitis, R. J. *J. Inorg. Biochem.* **2001**, *86*, 298. (c) Kong, D. Y.; Reibenspies, J.; Martell, A. E.; Motekaitis, R. J. *Inorg. Chim. Acta* **2001**, *324*, 35. (d) Wang, J.; Martell, A. E.; Motekaitis, R. J. *Inorg. Chim. Acta* **2001**, *322*, 47.

Chart 1. Drawings and Abbreviations of the Ligands Used in This Work

In this paper we report the host–guest binding interactions of the ligand 3,7,11,18,22,26-hexaazatricyclo[26.2.2.2^{13,16}]-tetratriaconta-1(31),13(34),14,16(33),28(32),29-hexaene (P3) with phosphate and diphosphate substrates and we compare them with the ones obtained by the isomeric ligand 3,7,11,19,23,27-hexaazatricyclo[27.3.1.1^{13,17}]tetratriaconta-1(33),-13,15,17(34),29,31-hexaene (Bn) (see Chart 1).

Those two isomeric ligands allow us to evaluate a fundamental feature of host–guest interactions such as the geometrical fit of the substrate with respect to the receptor, without any contamination from other receptor properties such as their basicity, Coulombic charge, or hydrogen-bonding capacity.

Experimental Section

Materials. GR grade KCl was obtained from Aldrich, and CO₂-free Dilut-it ampules of KOH were purchased from J. T. Baker Inc. Reagent grade potassium dihydrogen phosphate and tetrasodium diphosphate were purchased from Aldrich. The KOH solution was standardized by titration against standard potassium acid phthalate

with phenolphthalein as indicator and was checked periodically for carbonate content (<2%).¹⁰

3,7,11,18,22,26-Hexaazatricyclo[26.2.2.2^{13,16}]tetratriaconta-1(31),13(34),14,16(33),28(32),29-hexaene Hexahydrobromide [(H₆P3)Br₆]. A solution of 2.91 g (6.23 mmol) of the ligand P3 in 140 mL of 95% ethanol is prepared. The solution is kept under stirring in a ice bath, and 8 mL of 48% HBr (0.0702 mmol) is added dropwise. After complete addition, the solution is kept stirring for further 30 min. After that time, the solid obtained is filtered off the solution and washed with 95% ethanol. The solid is crystallized from hot water/methanol solution. Crystalline colorless needles are obtained after 48 h at 0 °C. After the needles are filtered off the solution, washed with methanol and diethyl ether, and dried, the yield is 65%. FT-IR (KBr): ν 1448, 2802, 1573, and 2953 cm⁻¹. ¹H NMR (D₂O, 200 MHz, 298 K, DSS_{int}): δ 7.56 (s, 8H, arom), 4.31 (s, 8H, Ar–CH₂), 3.04 (m, 16H, NCH₂CH₂CH₂N), 2.06 (m, 8H, NCH₂CH₂CH₂N). ¹³C NMR (D₂O, 50 MHz, 298 K, DSS_{int}): δ 134.56 (arom quat), 133.97 (arom terc), 53.40 (Ar–CH₂), 47.40, 45.97 (NCH₂CH₂CH₂N), 25.69 (NCH₂CH₂CH₂N). Anal. Calcd for C₂₈H₅₂N₆Br₆·4H₂O·C₄H₁₀O: C, 34.99; H, 6.42; N, 7.65. Found: C, 34.89; H, 6.48; N, 7.70.

Physical Methods. IR spectra were taken in a Mattson-Galaxy Satellite FT-IR spectrophotometer as solid KBr pellets. Elemental analyses were conducted in a Carlo Erba Instrument, model CHNS 1108. ¹H and ¹³C NMR spectra were recorded at 298 K in a Bruker DPX200 model Avance (4.7) operating at 200 MHz for proton. Spectra were referenced to TMS or DSS. ³¹P NMR spectra were measured at 202.45 MHz using a Bruker Avance 500 spectrometer equipped with a inverse triple-resonance probehead. A total of 128 scans were collected for each ¹D ³¹P spectrum acquired without ¹H NOE decoupling during the relaxation delay. FID were recorded with 8192 points and processed using an exponential window with a line broadening of 2 Hz. An external reference of 85% H₃PO₄ was used for calibration purposes.

Potentiometric Titrations. Potentiometric measurements were conducted in a jacketed cell thermostated at 25.0 °C and kept under an inert atmosphere of purified and humidified argon. For the potentiometric measures a Crison pHmeter (model 2002) was used equipped with a glass electrode and a Ag/AgCl reference electrode with saturated KCl as internal solution. The volume of titrating agent to be added to the reaction mixture is controlled by means of a electronic Crison buret with a nominal volume of 2.5 mL. The support electrolyte used to keep ionic strength constant at 0.10 M was KCl. The electrodes were calibrated by titrating a small amount of HCl at an ionic strength of 0.10 M and a constant temperature of 25 °C and determining the titration end point with the Gran¹¹ method that allows to calculate the electrode's standard potential (E°). $\log K_w$ for the system, defined in terms of $\log([H^+][OH^-])$, was found to be –13.78 at the ionic strength employed¹² and was kept fixed during refinements.

Acid dissociation constants for the phosphate and diphosphate anions were determined under exact conditions employed in this work and were found to agree well with data from the literature.¹²

Potentiometric measurements of solutions either containing the ligand or the ligand plus equimolecular amounts the appropriate phosphate or diphosphate anion were run at concentrations of 2.0 × 10⁻³ M and ionic strengths of $\mu = 0.10$ M (KCl). At least 10

- (4) (a) Bazzicalupi, C.; Bencini, A.; Bianchi, A.; Cecchi, M.; Escuder, B.; Fusi, V.; García-España, E.; Giorgi, C.; Luis, S. V.; Maccagni, C.; Marcelino, V.; Paoletti, P.; Valtancoli, B. *J. Am. Chem. Soc.* **1999**, *121*, 6807. (b) Doménech, A.; García-España, E.; Ramírez, J. A.; Celda, B.; Martínez, M. C.; Monleon, D.; Tejero, R.; Bencini, A.; Bianchi, A. *J. Chem. Soc., Perkin Trans. 2* **1999**, *1*, 23. (c) Aguilar, J. A.; Celda, B.; Fusi, V.; García-España, E.; Luis, S. V.; Martínez, M. C.; Ramírez, J. A.; Soriano, C.; Tejero, R. *J. Chem. Soc., Perkin Trans. 2* **2000**, *7*, 1323. (d) Arranz, P.; Bencini, A.; Bianchi, A.; Diaz, P.; García España, E.; Giorgi, C.; Luis, S. V.; Querol, M.; Valtancoli, B. *J. Chem. Soc., Perkin Trans. 2* **2001**, *9*, 1765. (e) Bazzicalupi, C.; Bencini, A.; Berni, E.; Bianchi, A.; Fornasari, P.; Giorgi, C.; Masotti, A.; Paoletti, P.; Valtancoli, B. *J. Phys. Org. Chem.* **2001**, *14*, 432. (f) Aguilar, J.; Díaz, P.; Escartí, F.; García-España, E.; Gil, L.; Soriano, C.; Begoña, V. *Inorg. Chim. Acta* **2002**, *339*, 307. (g) Escartí, F.; Miranda, C.; Lamarque, L.; LaTorre, J.; García-España, E.; Kumar, M.; Vicente J. A.; Navarro, P. *Chem. Commun.* **2002**, 936.
- (5) (a) Beer, P. D.; Shade, M. *Chem. Commun.* **1997**, *24*, 2377. (b) Beer, P. D.; Cadman, J.; Lloris, J. M.; Martínezmanez, R.; Soto, J.; Pardo, T.; Marcos, M. D. *J. Chem. Soc., Dalton Trans.* **2000**, *11*, 1805.
- (6) (a) Kanyo, Z. F.; Christianson, D. W. *J. Biol. Chem.* **1991**, *266*, 4264. (b) Alfonso, I.; Dietrich, B.; Rebolledo, F.; Gotor, V.; Lehn, J. M. *Helv. Chim. Acta* **2001**, *84*, 280. (c) Rivera, J. M.; Martin, T.; Rebek, J. *J. Am. Chem. Soc.* **2001**, *123*, 5213. (d) Choi, K. H.; Hamilton, A. D. *J. Am. Chem. Soc.* **2001**, *123*, 2456. Deetz, M. J.; Shukla, R.; Smith, B. D. *Tetrahedron* **2002**, *58*, 799. (e) Rekharsky, M. V.; Inoue, Y. *J. Am. Chem. Soc.* **2002**, *124*, 813. (f) McCleskey, S. C.; Griffin, M. J.; Schneider, S. E.; McDevitt, J. T.; Anslyn, E. V. *J. Am. Chem. Soc.* **2003**, *125*, 1114–1115.
- (7) Aoki, S.; Kimura, E. *Rev. Mol. Biotechnol.* **2002**, *90*, 129–155.
- (8) Christos A. I.; Steed, J. W. *J. Supramol. Chem.* **2001**, *1*, 165–187.
- (9) (a) Anda, C.; Lobet A.; Salvadó, V.; Reibenspies, J.; Martell, A. E.; Motekaitis, R. J. *Inorg. Chem.* **2000**, *39*, 2986. (b) Anda, C.; Lobet, A.; Salvadó, V.; Martell, A. E.; Motekaitis, R. J. *Inorg. Chem.* **2000**, *39*, 3000.

- (10) Martell, A. E.; Motekaitis, R. J. *Determination and Use of Stability Constants*, 2nd ed.; John Wiley and Sons: New York, 1992.

- (11) Gran, G. *Analyst (London)* **1952**, *77*, 661.

- (12) Smith, R. M.; Martell, A. E. *NIST Critically Selected Stability Constants: Version 2.0*; National Institute of Standards and Technology: Gaithersburg, MD, 1995.

points/neutralization of every hydrogen ion equivalent were acquired, repeating titrations until satisfactory agreement was obtained. A minimum of three consistent sets of data was used in each case to calculate the overall stability constants and their standard deviations. The range of accurate p[H] measurements was considered to be 2–12. Equilibrium constants and species distribution diagrams were calculated using the programs BEST¹³ and SPEXY, respectively.¹⁴

Crystal Structure Determination. Preparation of (H₆P3)Br₆·1/2H₂O·C₂H₆O. Small colorless crystals from P3·6HBr·1/2H₂O·C₂H₆O were obtained by slow diffusion in ethanol of a water solution of the hexabromated ligand adjusting the pH value at 3.02.

Data were collected at low-temperature $T = 180$ K on a Stoe imaging plate diffraction system (IPDS), equipped with an Oxford Cryosystems cryostream cooler device and using a graphite-monochromated Mo K α radiation ($\lambda = 0.71073$ Å). The final unit cell parameters were obtained by least-squares refinement of a set of 5000 well-measured reflections, and crystal decay was monitored by measuring 200 reflections by image; no significant fluctuations of intensities were observed during data collection. Semiempirical corrections for absorption¹⁵ were applied.

The structure was solved by direct methods using SIR92 and expanded by subsequent differences Fourier maps and then refined by least-squares procedures on F^2 with the aid of SHELXL97¹⁶ by minimizing the function $\sum w(F_o^2 - F_c^2)^2$, where F_o and F_c are respectively the observed and calculated structure factors. The atomic scattering factors were taken from ref 17. All hydrogen atoms were located on a difference Fourier maps, but the positional parameters of the hydrogens atoms were obtained geometrically using an idealized model and then the H atoms were refined using a riding model with an isotropic displacement parameter of 1.2 times the U_{eq} value of the attached C sp² and 1.5 times the U_{eq} value of the attached C sp³ atom; the methyl groups were refined with a rotation around the bond C–C as free variable. For the NH₂ groups the hydrogen atoms labeled H(1A), H(1B), H(2A), H(2B), H(3A), H(3B), H(4A), and H(4B) were isotropically refined with an isotropic parameter fixed at 1.2 times the U_{eq} value of the nitrogen atom to which they were connected. A statistic disorder was observed for one molecule of ethanol localized; the oxygen atom was found distributed on two different sites with a ratio of occupancy equal to 0.25:0.25.

All non-hydrogen atom were anisotropically refined, and in the last cycles of refinement a weighting scheme was applied, where weights have been calculated from the following formula:

$$w = 1/[\sigma^2(F_o^2) + (aP)^2 + bP]$$

Here $P = (F_o^2 + 2F_c^2)/3$.

Drawings of molecules are performed with the program ORTEP3¹⁸ with 50% probability displacement ellipsoids for non-hydrogen atoms.

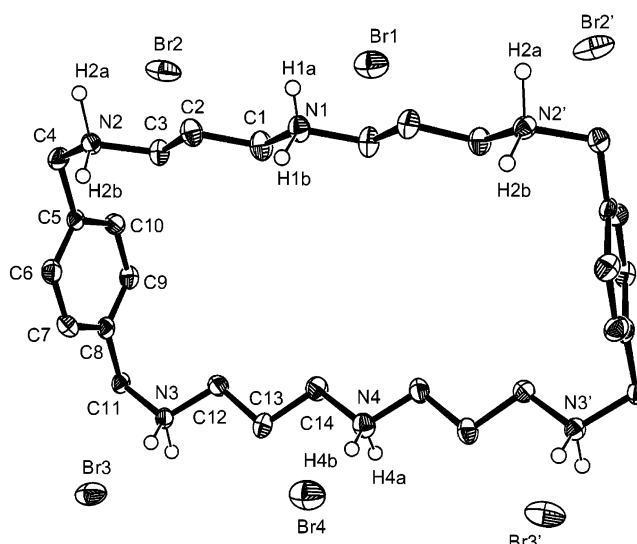


Figure 1. Thermal ellipsoid plot, 50% probability, of (H₆P3)Br₆ including the atomic labeling scheme.

Table 1. Summary of Crystal Structure Results

empirical formula	C ₂₈ H ₅₂ N ₆ Br ₆ ·0.5H ₂ O·C ₂ H ₅ OH
fw	1007.28
cryst system	monoclinic
space group	$P2_1/m$
a , Å	7.4653(4)
b , Å	30.4519(3)
c , Å	10.7740(7)
β , deg	110.064(7)
V , Å ³	2305.7(3)
formula units/cell	2
temp, K	180(2)
λ (Mo K α), Å	0.71073
ρ_{calc} , g/cm ³	1.451
μ , mm ⁻¹	5.252
R^a	0.045
R_w^b	0.122

$$^a R = \sum |F_o| - |F_c| / \sum |F_o|, \quad ^b R_w = [\sum [w(F_o^2 - F_c^2)^2] / \sum [w(F_o^4)]]^{1/2}.$$

Results and Discussion

Synthesis and Structure of (H₆P3)Br₆. The P3 ligand was prepared by following literature procedures or slight modifications thereof,^{19,20} while its corresponding hexabromide salt was synthesized for the first time by treating P3 with 48% HBr. The crystal structure of (H₆P3)Br₆ was determined by X-ray diffraction analysis, and its ORTEP diagram is shown in Figure 1. Table 1 presents its crystallographic data whereas bond distances and angles, including hydrogen bonding, are displayed as Supporting Information. The metric parameters obtained for (H₆P3)Br₆·1/2H₂O·C₂H₆O are within the expected values for this type of compound.²⁰ The compound has a plane of symmetry perpendicular to the ligand cavity that contains N1 and N4. The planes described by the aromatic rings present an angle of 19.12° while the angle formed by the cavity and the aromatic rings is of 80.39°. The macrocyclic cavity can be described as a 12.4 × 5.8 Å² rectangle which is roughly 12%

(19) Pietraszkiewicz, M.; Gasiorowski, R. *Chem. Ber.* **1990**, *123*, 405.

(20) Llobet, A.; Reibenspies, J.; Martell, A. E. *Inorg. Chem.* **1994**, *33*, 5946.

(13) Martell, A. E.; Motekaitis, R. J. *Determination and Use of Stability Constants*, 2nd ed.; John Wiley and Sons: New York 1992.

(14) SPEXY is a program created by R. J. Motekaitis which generates an X–Y file that contains the concentration of all the existent species in solution as a function of p[H] using BEST output files.

(15) DIFABS. Walker, N.; Stuart, D. *Acta Crystallogr., Sect A* **1983**, *39*, 158–166.

(16) Sheldrick, G. M. *SHELXL97. Program for the Refinement of Crystal Structures*; University of Göttingen: Göttingen, Germany, 1997.

(17) *International Tables for X-ray Crystallography*; Kynoch Press: Birmingham, England, 1974; Vol. IV.

(18) ORTEP3 for Windows. Farrugia, L. J. *J. Appl. Crystallogr.* **1997**, *30*, 565.

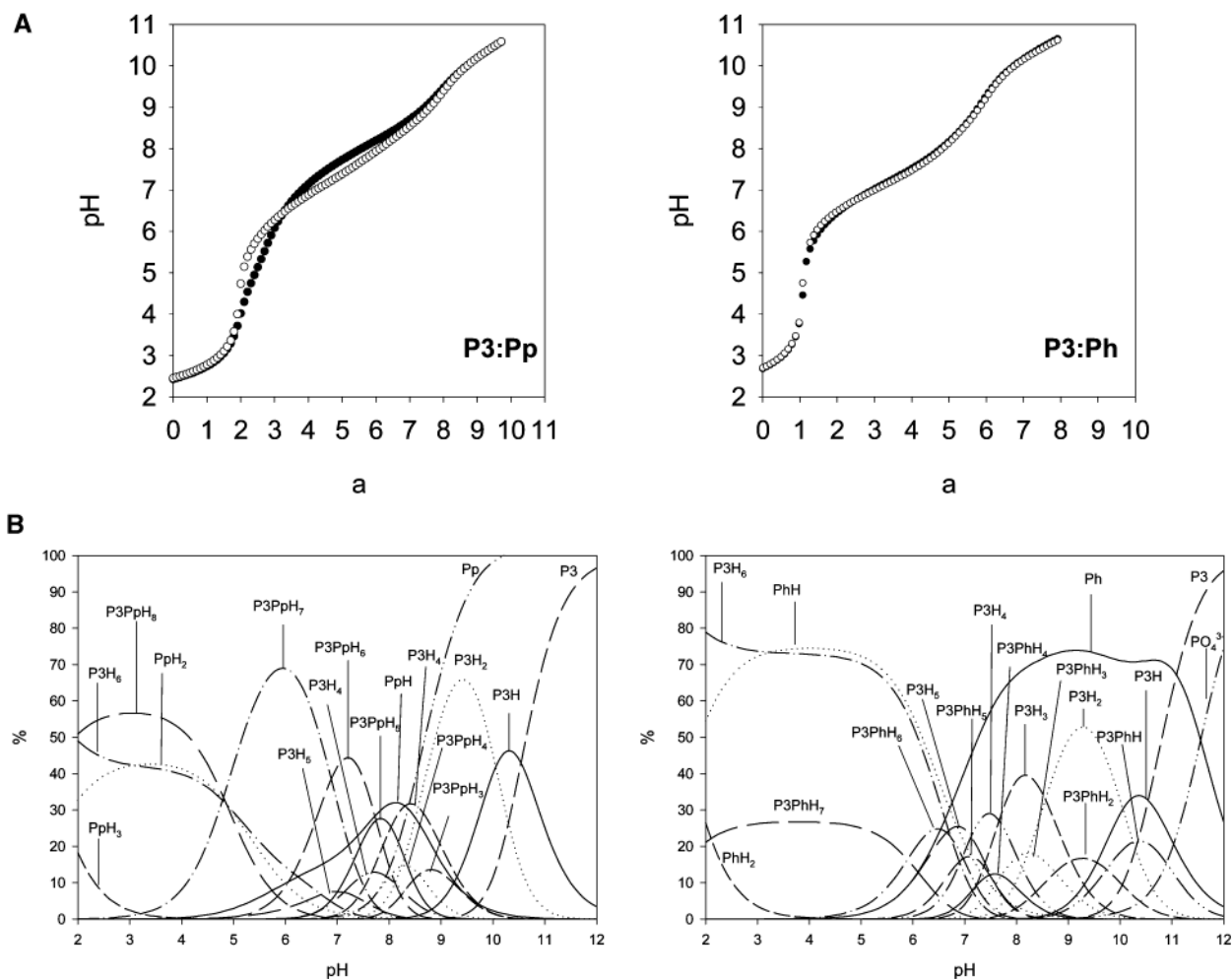


Figure 2. (A) (●) Experimental curves obtained for the potentiometric titrations of equilibrated diphosphate (left) and monophosphate (right) (2.0×10^{-3} M) with the ligand H_6P3^{6+} (2.0×10^{-3} M) at 25.0 °C and $\mu = 0.1$ M (KCl) and (○) calculated potentiometric curve for the same system assuming there is no interaction between the substrate and the ligand. (B) Species distribution diagram as a function of $p[H]$ for the P3–Pp and P3–Ph systems.

Table 2. Logarithms of the Protonation Constants of P3 and Bn Ligands (L) and Phosphate and Diphosphate Substrates (S) at 25.0 °C and $\mu = 0.10$ M (KCl) With Charges Omitted for Clarity

equilibr quotient (L)	P3 ^a	Bn	equilibr quotient (S)	Pp ^a	Ph ^a
$K^H_1 = [HL]/[L][H]$	10.55	10.33	$K^H_1 = [HS]/[S][H]$	8.36	11.56
$K^H_2 = [H_2L]/[HL][H]$	10.06	9.73	$K^H_2 = [H_2S]/[HS][H]$	5.99	6.71
$K^H_3 = [H_3L]/[H_2L][H]$	8.56	8.56	$K^H_3 = [H_3S]/[H_2S][H]$	1.75	1.69
$K^H_4 = [H_4L]/[H_3L][H]$	7.67	7.77			
$K^H_5 = [H_5L]/[H_4L][H]$	7.12	7.22			
$K^H_6 = [H_6L]/[H_5L][H]$	6.70	6.64			
$\Sigma \log K^H_i$	50.64	50.24			
$1000\sigma_{fit}$ or ref	1.9	9a		2.2	4.5

^a This work.

larger than for the related *meta* isomer, H_6Bn^{6+} ($12.8 \times 4.9 \text{ \AA}^2$), due to the increase of two member ring units (28 for Bn; 30 for P3).

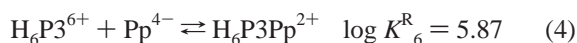
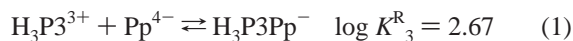
Recognition Capacity of the P3 Ligand. Potentiometric titrations of H_6P3^{6+} allow one to measure its six protonation constants that, as expected, are extremely similar to those of H_6Bn^{6+} as shown in Table 2.^{9a,20} The experimental curve as well as the corresponding species distribution diagram as a function of $p[H]$ is shown as Supporting Information. Phosphate and diphosphate anionic complex formation with P3 and its different protonated forms were also calculated

Table 3. Stepwise Association Constants (K) for the Interaction of P3 and Bn with S ($S = Pp$ and Ph ; $Ph = HPO_4^{2-}$) at 25.0 °C and $\mu = 0.10$ M (KCl) With Charges Omitted for Clarity

ratio L:S:H	equilibr	diphosphate (Pp)		phosphate (Ph)	
		P3	Bn	P3	Bn
1:1:1	$[HLS]/[HL][S]$			2.65	
1:1:2	$[H_2LS]/[H_2L][S]$			2.33	
1:1:3	$[H_3LS]/[H_3L][S]$	2.67	2.57	2.52	
1:1:4	$[H_4LS]/[H_4L][S]$	3.58	4.12	2.57	2.13
1:1:5	$[H_5LS]/[H_5L][S]$	4.81	6.13	2.92	2.96
1:1:6	$[H_6LS]/[H_6L][S]$	5.87	7.85	3.20	3.50
1:1:7	$[H_7LS]/[H_6L][HS]$	4.39	5.25	2.39	
1:1:8	$[H_8LS]/[H_6L][H_2S]$	3.20	2.93		
	$1000\sigma_{fit}$ or ref	3.2	9a	7.8	9a

using the same technique. The experimental curves are displayed in Figure 2A. The mathematical treatment allows one to fully characterize the different equilibria present in solution, and the results obtained are presented in Table 3. As expected from the larger deviation of the potentiometric curves, with regard to the noninteraction situation (see Figure 2A), in the case of the diphosphate substrate it yields much stronger log of recognition constants than in the case of the monophosphate substrate.

For the P3–Pp system ($\sigma_{\text{fit}} = 0.0032$) the presence of six equilibrium species is detected, which are expressed as follows:



Here K^{R}_i is the recognition constant of protonation degree i and they are listed in order of appearance from low to high $\text{p}[\text{H}]$.

Figure 2B displays the species distribution diagram for this type of ternary systems. In the case of the P3/Pp/H system, the complexed species have always higher concentrations than free Pp ligand or its different protonated species within the pH range 2–8.5. This is a further indication of the strength of the formed ternary species in this particular system. In sharp contrast for the P3/Ph/H system the ligand-based species dominate always over the whole pH range, thus indicating the weakness of the corresponding ternary species.

The recognition constant values obtained for this system lay within the range of previously reported host–guest interactions with hexaaza macrocyclic amines and phosphates containing aromatic^{9a,20,21,22} and aliphatic²³ spacers.

The highest equilibrium constant for the present ternary recognition complexes P3/Pp/H corresponds to the formation of the species $\text{H}_6\text{P3Pp}^{2+}$, $\log K^{\text{R}}_6 = 5.87$. This complex can be formally described as a H_6P^{6+} positive cation bonded to a Pp^{4-} anion by Coulombic forces and hydrogen bonds. In this complex the Coulombic interactions and hydrogen bonding reach a maximum.

If one takes into consideration that the first protonation constant of Pp^{4-} is 8.42 (Table 2), which is higher than the sixth protonation constants of P3 (6.70, Table 2), and that the fifth, fourth, and third P3 protonation constants are

relatively close, there is another possible set of equilibria that can lead to the formation of H_iPnPp ($i = 3–6$) ternary species:



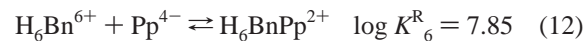
For each species both equilibria simultaneously operate and their relative importance is a function of $\text{p}[\text{H}]$. Similar arguments can be used to propose the following alternative equilibrium for the formation of $\text{H}_7\text{P3Pp}^{3+}$:



The extremely good reproducibility of the systems described above is an excellent indication that no further process are taking place but the recognition phenomena. Nevertheless, it has been described in the literature that related polyammonium macrocycles might be active with regard to polyphosphate and/or nucleotide hydrolysis especially at the temperatures 80–100 °C.²⁴ Thus, we checked the Bn–Pp system at pH 6.0 and 3.0 at room temperature for 24 h, through ³¹P NMR, and we did not find any hydrolysis at all (the resonances $\delta = -9.6$ ppm, pH = 6.0, and $\delta = -9.8$ ppm, pH = 3.0, do not change over the 24 h) in agreement with the excellent reproducibility of the potentiometric experiments.

Competitive Diagrams and Selectivity. Figure 3A shows a graphical representation of the different recognition constants as a function of proton content obtained for the P3/Pp/H and the Bn/Pp/H ternary systems. Bn is the isomeric ligand shown in Chart 1, where the aromatic rings are linked in the *meta* position in lieu of the *para* position (its numerical values are shown in Tables 2 and 3 for the stepwise ligand protonation constants and for the recognition constants with the Pp and Ph substrates, respectively).

For the ternary systems with the diphosphate substrate it is found that in most cases the Bn ligand forms stronger complexes than with the P3 ligand. In the particular case of K^{R}_6 they differ in nearly 2 orders of magnitude as displayed in the eqs 4 and 12.



As a consequence of this, the competitive distribution diagram, Figure 4, shows a strong predominance of the Bn/Pp/H over the P3/Pp/H ternary species (from pH 3.5 to 10). At pH 7.4, for instance, the selectivity of Bn-containing species over P3 is 88.8% (the selectivity for Bn-containing species over P3 at a particular pH is defined according to the following equation: $[\sum_i(\% \text{H}_i/\text{Bn}/\text{Pp})]/(\sum_i(\% \text{H}_i/\text{Bn}/\text{Pp}))$)

- (21) (a) Lu, Q.; Motekaitis, R. J.; Reibenspies, J. H.; Martell, A. E. *Inorg. Chem.* **1995**, *34*, 4958. (b) Motekaitis, R. J.; Martell, A. E. *Inorg. Chem.* **1992**, *31*, 5534.
- (22) (a) Nation, D. A.; Martell, A. E.; Carroll, R. I.; Clearfield, A. *Inorg. Chem.* **1996**, *35*, 7246. (b) Lu, Q.; Reibenspies, J. H.; Carroll, R. I.; Martell, A. E.; Clearfield, A. *Inorg. Chim. Acta* **1998**, *270*, 207. (c) Lu, Q.; Reibenspies, J. H.; Martell, A. E.; Motekaitis, R. J. *Inorg. Chem.* **1996**, *35*, 2630. (d) Bazzicalupi, C.; Bencini, A.; Bianchi, A.; Fusi, V.; Giorgi, C.; Granchi, A.; Paoletti, P.; Valtancoli, B. *J. Chem. Soc., Perkin Trans. 2* **1997**, 775.
- (23) (a) Hosseini, M. W.; Lehn, J.-M. *Helv. Chim. Acta*, **1987**, *70*, 1312. (b) Jurek, P. E.; Martell, A. E.; Motekaitis, R. J.; Hancock, R. D. *Inorg. Chem.* **1995**, *34*, 1823. (c) Motekaitis, R. J.; Martell, A. E. *Inorg. Chem.* **1994**, *33*, 1032. (d) English, J. B.; Martell, A. E.; Motekaitis, R. J.; Murase, I. *Inorg. Chim. Acta*, **1997**, *258*, 183. (e) Dietrich, B.; Hosseini, M. W.; Lehn, J.-M. *Helv. Chim. Acta*, **1985**, *68*, 289. (f) Motekaitis, R. J.; Martell, A. E. *Inorg. Chem.* **1982**, *60*, 2403.

- (24) Andres, A.; Arago, J.; Bencini, A.; Bianchi, A.; Domenech, A.; Fusi, V.; Garcia-España, E.; Paoletti, P.; Ramirez, A. *Inorg. Chem.* **1993**, *32*, 3418.

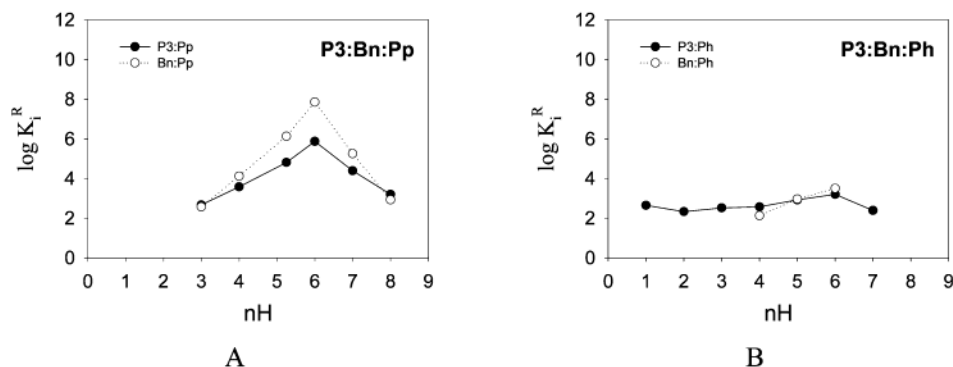


Figure 3. Plot of $\log K_i^R$ versus nH (the different ternary species with various degree of protonation) for (A) the P3–Pp and Bn–Pp systems and (B) the P3–Ph and Bn–Ph systems.

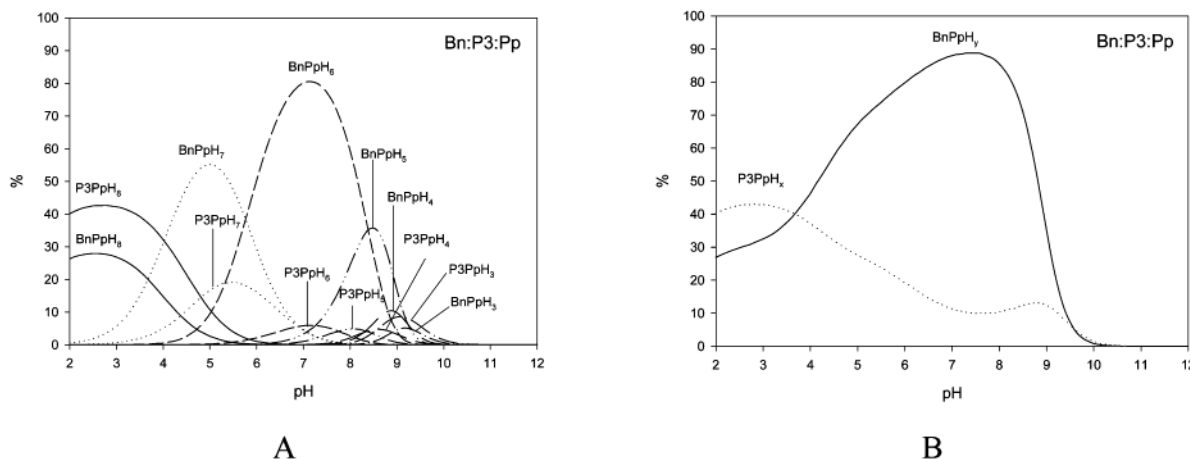


Figure 4. (A) Competitive calculated species distribution diagram for systems with equimolar amounts of the Bn and P3 ligands and diphosphate. (B) Corresponding total species distribution diagram.

+ $\sum_i(\% H_i/P3/Pp)] \times 100$). In sharp contrast for the ternary systems with the monophosphate substrate the binding constants are very similar and thus independent of the ligand.

The results just described here for the formation of anionic complexes with the diphosphate substrate clearly indicate that the Bn ligand is capable of stronger recognition of this substrate compared to its isomeric P3 ligand. This recognition capacity, given the similarity in the chemical nature of Bn and P3, arises only because of the different shape and/or size of the cavity of those two ligands. Thus the Bn ligand, which has a smaller and more rectangular cavity than its P3 isomer, is capable of better fitting the diphosphate substrate and thus ends up forming much more stronger complexes. This is further corroborated by the behavior of those two ligands with regard to the monophosphate substrate. In this particular case, the substrate binds to the ligands in a very similar manner, since the smaller size of the monophosphate

substrate cannot be discriminated by the large cavities of those hexaazamacrocyclic ligands.

Acknowledgment. This research has been financed by the MCYT of Spain through Project BQU2000-0458. A.L. is grateful to the CIRIT Generalitat de Catalunya (Spain) for the Distinction award and the aid of Grant SGR2001-UG-291. C.A. thanks the University of Girona for the allocation of a doctoral grant.

Supporting Information Available: A CIF file for (H₆P3)Br₆ with CCDC number 223738 together with a table containing bond distances and angles, including hydrogen bonding, for this crystal, experimental potentiometric curves, and species distribution diagrams as a function of $p[H]$ obtained for this ligand. This material is available free of charge via the Internet at <http://pubs.acs.org>. IC034205V